RAPID COMMUNICATIONS

PHYSICAL REVIEW E VOLUME 51, NUMBER 2 FEBRUARY 1995

Theory of chiral defects in Langmuir monolayers

J. V. Selinger
Center for Bio/Molecular Science and Engineering, Naval Research Laboratory, Code 6900, 4555 Overlook Avenue, SW, Washington, DC 20375

R. L. B. Selinger*
Institute for Physical Science and Technology, University of Maryland, College Park, Maryland 20742
(Received 8 August 1994)

Thin films often exhibit a spontaneous breaking of chiral symmetry. This symmetry breaking can occur on two distinct length scales. On a microscopic scale, nonchiral molecules can pack in a chiral structure. On a macroscopic scale, a striped texture can buckle to form a spiral. Using continuum elastic theory and Monte Carlo simulations, we predict the defect textures that result from macroscopic chiral symmetry breaking and contrast them with earlier predictions for microscopic symmetry breaking. We identify experiments in which each type of symmetry breaking occurs.

PACS number(s): 61.30.Jf, 64.70.Md, 68.10.−m, 68.15.+e

Thin films of organic molecules exhibit many types of order and many types of modulated structures on different length scales [1]. In addition to tilt order, bond-orientational order, and crystalline order, several recent experiments have found *chiral order* in thin films of nonchiral molecules. Atomic force microscopy has explicitly shown local chiral order in Langmuir-Blodgett films [2,3]. Optical microscopy has shown chiral textures in liquid-crystal films [4,5] and Langmuir monolayers [6–8], which indicate that the films have spontaneously broken chiral symmetry. To describe these textures, Selinger, Wang, Bruinsma, and Knobler (SWBK) [9] proposed a general theory of chiral symmetry breaking on a microscopic length scale. This theory is based on a local chiral order parameter, which is coupled to bend deformations in the molecular tilt orientation. The textures predicted by this theory are consistent with experiments on freely suspended films of smectic liquid crystals. However, there are substantial inconsistencies between the predicted textures and experiments on Langmuir monolayers. As discussed below, Langmuir monolayers exhibit a chiral symmetry breaking that cannot be explained through this model of local chiral order.

In this paper, we present an alternative model for chiral symmetry breaking that can explain these experiments on Langmuir monolayers. The essence of our model is that a striped texture, which forms for reasons unrelated to chirality, can buckle in the presence of a point defect to form a spiral. This buckling process breaks chiral symmetry on the macroscopic (50 μm) length scale of the defect texture, but not on the microscopic (5 Å) length scale of the molecular packing. Thus thin films can develop chiral order on either length scale. Our distinction between microscopic and macroscopic chiral symmetry breaking is similar to the distinction between spontaneous and induced chirality proposed by Kaganer and Loginov [10], but we emphasize the length scale of chiral order. Our results show that a full description of these films must include ordering over a wide range of length scales.

To describe chiral symmetry breaking on a microscopic length scale, SWBK developed a theory based on a local chiral order parameter $\psi(\mathbf{r})$, which gives the magnitude and sign of chiral symmetry breaking. For example, if chiral symmetry is broken by the phase separation of a racemic mixture, $\psi(\mathbf{r})=\rho_R(\mathbf{r})-\rho_L(\mathbf{r})$ is the difference in densities of the right- and left-handed enantiomers. This chiral order parameter is coupled to variations in the direction of molecular tilt. A general free energy can be written as

$$F=\int d^2\mathbf{r}[\tfrac{1}{2}\kappa(\nabla\psi)^2+\tfrac{1}{2}t\psi^2+\tfrac{1}{4}u\psi^4+\tfrac{1}{2}K_1(\nabla\cdot\mathbf{c})^2 + \tfrac{1}{2}K_3(\nabla\mathbf{c})^2-\lambda\psi\hat{\mathbf{z}}\cdot\nabla\times\mathbf{c}]. \quad (1)$$

Here, $\mathbf{c}(\mathbf{r})$ gives the direction of molecular tilt, projected into the layer plane. In this model, the tilt magnitude $|\mathbf{c}|$ is assumed to be constant. The first three terms are the Ginzburg-Landau expansion in powers of ψ. The next two terms are the Frank free energy for splay and bend of $\mathbf{c}$. The final term is the coupling between ψ and $\mathbf{c}$. It is permitted by symmetry because both ψ and $\hat{\mathbf{z}}\cdot\nabla\times\mathbf{c}$ change sign under reflection. Using mean-field theory, SWBK derived the phase diagram for this model. The phase diagram shows a uniform nonchiral phase for high temperature t and a uniform chiral phase for low t. For intermediate t, there are two modulated phases: a striped phase and a square lattice. In the striped phase, there are alternating stripes of positive and negative chirality. In each stripe of positive chirality, $\mathbf{c}$ bends counterclockwise, and in each stripe of negative chirality, $\mathbf{c}$ bends clockwise. In the square-lattice phase, there are alternating cells of positive and negative chirality, which give alternating vortices and antivortices in $\mathbf{c}$.

This theory of chiral symmetry breaking on a microscopic length scale is at least qualitatively consistent with experiments on freely suspended liquid-crystal films by Pang and Clark [5]. These experiments show a transition from a uniform nonchiral phase to a striped phase, characterized by a spontaneous bend in $\mathbf{c}$. The sign of the bend alternates be-

*Present address: Materials Science and Engineering Laboratory, National Institute of Standards and Technology, Gaithersburg, MD 20899.

tween clockwise and counterclockwise in successive stripes. The stripe width diverges at the phase transition, in agreement with the theoretical prediction of critical behavior. By contrast, there are significant inconsistencies between the textures predicted by this theory and experiments on Langmuir monolayers of fatty acids. Recent experiments [7,8] have shown that the director modulation in these monolayers is splay rather than bend. Moreover, neighboring stripes are identical; there is no alternation between successive stripes. Nevertheless, these Langmuir monolayers do exhibit chiral symmetry breaking, as seen in their spiral textures. Thus these systems must exhibit a different type of chiral symmetry breaking, which cannot be described by a local chiral order parameter.

To explain these experiments on Langmuir monolayers, we propose a model for chiral symmetry breaking on a macroscopic length scale. This model is based on an alternative mechanism for striped textures in monolayers. Several investigators have shown that stripes can be induced by the asymmetry between molecular heads and tails in monolayers, even without any chirality. This effect was studied in the context of liquid-crystal surfaces by Meyer and Pershan [11]. For Langmuir monolayers, this effect has been studied in a molecular model by Safran *et al.* [12], and in a continuum model by Hinshaw *et al.* [13] and Jacobs *et al.* [14]. In the molecular point of view, the molecular heads and tails take up different amounts of area, and hence the most efficient packing leads to a splay between the orientations of neighboring molecules. In the continuum perspective, the head-tail asymmetry permits terms of the form $\nabla\cdot\mathbf{c}$ or $|\mathbf{c}|^2\nabla\cdot\mathbf{c}$ in the free energy. Because $\nabla\cdot\mathbf{c}$ is a total divergence, its integral can be reduced to a surface integral, which depends only on boundary conditions. However, $|\mathbf{c}|^2\nabla\cdot\mathbf{c}$ is not a total divergence if $|\mathbf{c}|$ is not constant. The free energy can be therefore written as

$$F=\int d^2\mathbf{r}[-\tfrac{1}{2}a|\mathbf{c}|^2+\tfrac{1}{4}b|\mathbf{c}|^4+\tfrac{1}{2}K_1(\nabla\cdot\mathbf{c})^2 + \tfrac{1}{2}K_3(\nabla\times\mathbf{c})^2-\lambda_S|\mathbf{c}|^2\nabla\cdot\mathbf{c}]. \quad (2)$$

In this expression, the first two terms favor the tilt magnitude $|\mathbf{c}|=(a/b)^{1/2}$. The next two terms give the Frank free energy penalty for splay and bend of $\mathbf{c}$, as in Eq. (1). The final term, permitted by the head-tail asymmetry, favors a splay of $\mathbf{c}$. The coefficient λ_S is a measure of this asymmetry. The competition between the λ_S and K_1 terms determines the optimal splay.

The mean-field phase diagram for this model has been investigated in Refs. [13,14]. As λ_S increases, there is a transition from a uniform phase to a striped phase, shown schematically in Fig. 1(a). Within each stripe, there is a splay in $\mathbf{c}$. Between successive stripes, there is a sharp domain wall in which the magnitude of $\mathbf{c}$ is reduced while the direction of $\mathbf{c}$ rotates back. All of the stripes are identical; there is no alternation between successive stripes. The domain-wall width can be estimated as $\xi\approx(K_1/a)^{1/2}$, while the domain-wall energy per unit length is $E_{\rm wall}\approx(a^2/b)(K_1/a)^{1/2}$. The stripe width is then

$$w\approx K_1/(\lambda_S-E_{\rm wall}). \quad (3)$$

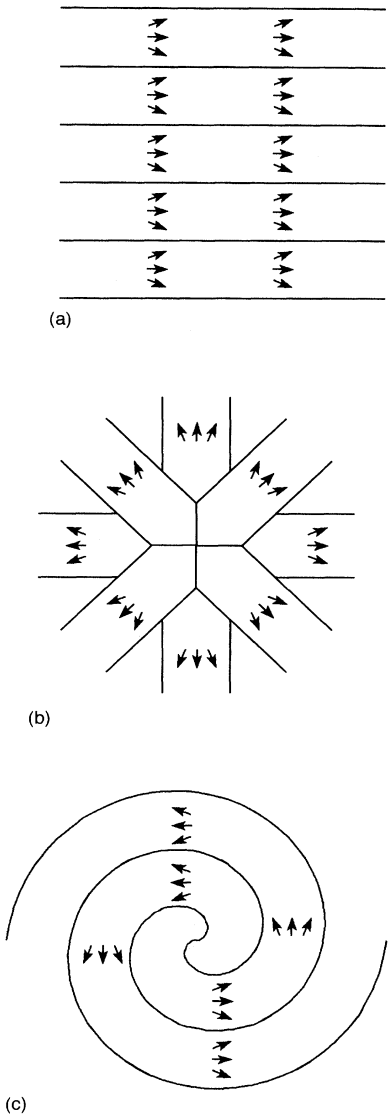

FIG. 1. Schematic views of (a) the striped phase, (b) a vortex defect with a dense branching morphology, and (c) a spiral defect. The arrows show $\mathbf{c}$, the direction of molecular tilt projected into the layer plane. Note that the spiral defect breaks chiral symmetry, while the striped phase and the dense branching morphology do not.

Recent experiments have shown that the striped textures observed in Langmuir monolayers are indeed consistent with the splay stripes predicted by this model [8]. The typical stripe width is $w\approx 50\ \mu$m.

The striped phase of Refs. [13,14] is the ground state of this model, and it is not chiral. In this paper, we point out that chiral symmetry can be spontaneously broken in the *defects* of the striped phase. Suppose there is a point vortex in $\mathbf{c}$. A point vortex could arise from (a) a localized impurity, (b) the kinetics of formation of the monolayer, (c) boundary conditions on a circular droplet, or (d) thermal fluctuations that nucleate a vortex-antivortex pair. Near the vortex core, there is more than the optimal splay. Away from the vortex core, the splay $\nabla\cdot\mathbf{c}$ decreases as $1/r$, where r is the distance from the core. As a result, the defect generates domain walls,

analogous to the walls in the periodic striped pattern, and thereby increases the splay up to the optimal value. Farther from the vortex core, the splay continues to decrease, or equivalently, the distance between the domain walls increases linearly with r. To maintain the optimal splay, the system may do either of two things. First, the defect may continue to generate more domain walls in a dense branching morphology, as shown in Fig. 1(b). Second, the pattern of domain walls may buckle to form a spiral, which maintains a constant spacing between walls, as in Fig. 1(c). If it forms a spiral, the handedness of the spiral is random. Equal numbers of right- and left-handed spirals should be formed, with the same free energy. Thus the formation of spiral defects leads to chiral symmetry breaking on the macroscopic length scale w of the splay stripes, even without any microscopic chiral order.

To determine whether the dense branching morphology or the spiral is the lower-energy defect, we estimate the energy of each texture. For the dense branching morphology, the main energy cost (compared to the periodic striped state) is the energy $E_{\rm disl}$ of each point dislocation where a domain walls begins. At the radius r from the defect core, the number of domain walls scales as r/w. Hence, in the annulus from r to $r+dr$, the number of dislocations scales as dr/w, and the dislocation density scales as $1/rw$. The energy of the dense branching morphology (DBM) therefore scales as

$$E_{\rm DBM} \approx \int_a^R r dr \, \frac{E_{\rm disl}}{rw} \approx \frac{E_{\rm disl} R}{w} , \tag{4}$$

where R is the system size and a the dislocation core radius. By contrast, the main energy cost of the spiral (compared to the periodic striped state) is the domain-wall curvature energy. Because the domain-wall curvature scales as $1/r$, the energy of the spiral scales as

$$E_{\rm spiral} \approx \int_a^R r dr \, \frac{\kappa}{r^2} \approx \kappa \ln \frac{R}{a} , \tag{5}$$

where κ is the domain-wall curvature rigidity. For large R, $E_{\rm spiral}$ grows less rapidly than $E_{\rm DBM}$. Thus the spiral is the lower-energy vortex defect.

Three other features of our model should be pointed out. First, the energy of a spiral defect depends only weakly on the number of spiral arms. The same stripe width can be achieved by spirals with fewer arms wound more tightly or more arms wound less tightly. Away from the vortex core, these configurations have the same energy density. The only small differences in energy are due to the structure close to the vortex core, which cannot be estimated well using continuum elastic theory. Thus spirals with different numbers of arms may coexist in the same monolayer. In experiments, spirals with 1 to 10 arms have been observed [7]. Second, a system of concentric circular stripes is a degenerate case of the spiral defect. The energy of a concentric defect is the same as a spiral, except for a small difference due to the core structure. Concentric defects have not been seen in experiments. Third, if a monolayer is compressed or dilated, all of the parameters in the free energy (2) change continuously, and hence the stripe width w changes continuously. In response to this change in w, all the spirals in the monolayer will become tighter or looser by winding or unwinding. To

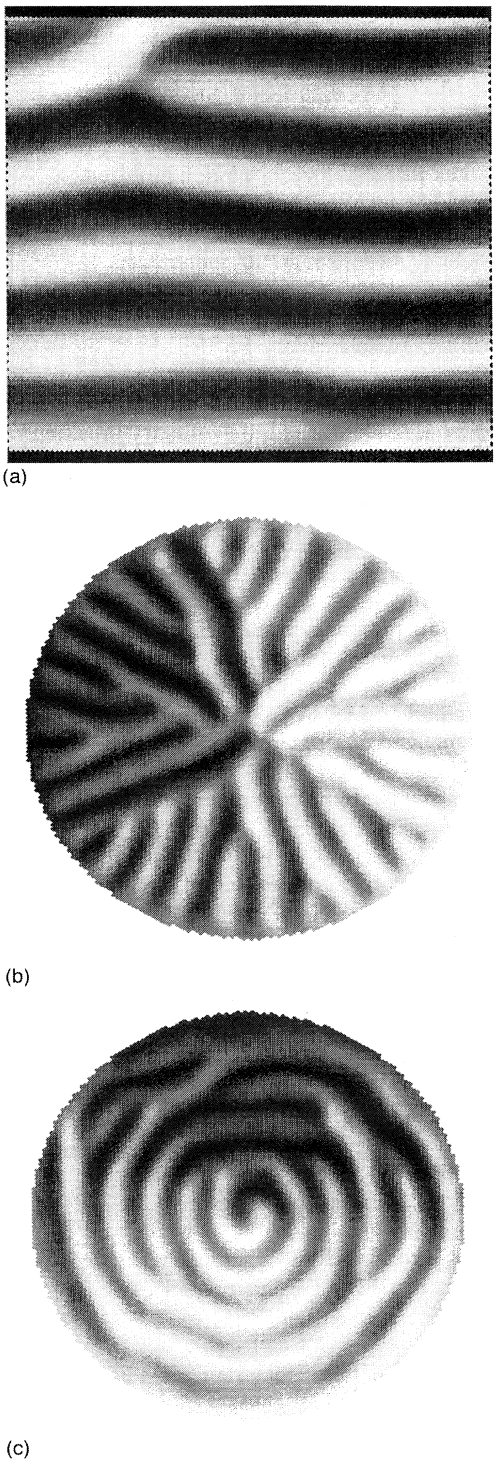

FIG. 2. Monte Carlo simulations of (a) the striped phase, (b) a vortex defect with a dense branching morphology, and (c) a spiral defect. The gray scale shows the y component of $\mathbf{c}$. Simulation (a) was done on a hexagonal lattice of 100×110 sites with periodic boundary conditions; (b) and (c) were done on a hexagonal lattice with a circular geometry with a radius of 85 sites.

change the spacing between arms, right- and left-handed spirals will rotate in opposite directions. This rotation has been observed experimentally [7].

As an explicit test of this analysis, we have performed Monte Carlo simulations of this model of Langmuir monolayers. In these simulations, we discretize the monolayer on a hexagonal lattice, with a director $\mathbf{c}_i$ defined on each site i. We make the approximation $K_1 = K_3 \equiv K$. The discretized free energy then becomes

$$F = \sum_{\langle i,j \rangle} [\tfrac{1}{2}K(\mathbf{c}_j - \mathbf{c}_i)^2 - \tfrac{1}{2}\lambda_S \hat{\mathbf{r}}_{ij} \cdot (\mathbf{c}_j - \mathbf{c}_i)(|\mathbf{c}_i|^2 + |\mathbf{c}_j|^2)] + \sum_i [-\tfrac{1}{2}a|\mathbf{c}_i|^2 + \tfrac{1}{4}b|\mathbf{c}_i|^4]. \quad (6)$$

In the simulations, we require $|\mathbf{c}_i| \leq 1$. This constraint is physically reasonable because $\mathbf{c}_i$ is the projection of a three-dimensional molecular director into the monolayer plane. Without this constraint, the free energy gives unphysical results: near a vortex, where $\nabla \cdot \mathbf{c}$ diverges, $|\mathbf{c}|$ becomes arbitrarily large and the vortex free energy becomes arbitrarily large and negative. (This problem was not considered in Refs. [13,14], because those papers did not investigate vortices.) In the simulations presented here, we use $K = \lambda = a = 1$ and $b = 2$. We begin the simulations with either a uniform director field or a single vortex. The temperature is initially set to 0.1, low enough that the system does not completely disorder but high enough that the system can relax to a lower-energy state. The temperature is slowly reduced to 0.001 or lower, in order to determine the ground state and low-lying defect states.

The simulation results are shown in Figs. 2(a)–2(c). In these figures, the gray scale indicates the y component of $\mathbf{c}$, with white representing positive values and black negative. This method of visualization is chosen because the gray scale approximately corresponds to the experimental fluorescence intensity in Refs. [6–8]. In Fig. 2(a), the simulation is done in a system with periodic boundary conditions. Initially, all the tilts are aligned along the x direction with magnitude $1/\sqrt{2}$. The system relaxes to the state of splay stripes, as expected from Refs. [13,14], with an energy per site of -0.1287. In Fig. 2(b), the simulation is done in a circular geometry, with boundary conditions favoring radial alignment of the tilts. Initially, all the tilts are aligned in the radial direction, with a vortex at the origin. This system relaxes to the dense branching morphology predicted in Fig. 1(b), with an energy per site of -0.1143. In Fig. 2(c), the simulation is again done in a circular geometry, but here the boundary conditions favor tangential alignment of the tilts, and all the tilts are initially aligned in the tangential direction. This system relaxes to the spiral state predicted in Fig. 1(c). The energy per site is -0.1258, lower than the dense branching morphology. This result confirms that the spiral is the lower-energy form of the vortex defect, and the dense branching morphology is only a metastable form. In these simulations, the striped texture and the spiral have some dislocations, which are not observed in experiments. Apparently these dislocations anneal away on experimental time scales, but do not have time to anneal away in the simulations.

The spiral defects discussed here are related to chiral defects that have been seen in liquid-crystal films. Dierker, Pindak, and Meyer [15] have observed analogous spiral defects in freely suspended smectic films of chiral liquid crystals. However, the spirals in those systems involve bend rather than splay of the director. That bend is induced by molecular chirality rather than by chiral symmetry breaking. Lavrentovich and Pergamenshchik [16] have observed spontaneous twist deformations in thick nematic films of nonchiral liquid crystals on liquid surfaces. The mechanisms that drive these spontaneous twist deformations are different from the mechanism for spiral formation discussed in this paper. However, these spontaneous twist deformations are also examples of chiral symmetry breaking on the macroscopic length scale of director modulations.

In conclusion, we have shown that chiral symmetry breaking can occur on two distinct length scales. On the microscopic length scale of molecular packing, nonchiral molecules can pack in a chiral structure, leading to the chiral textures predicted by SWBK. By contrast, on the much longer length scale of director modulations, a nonchiral pattern of splay stripes can buckle to form a spiral. Both types of chiral symmetry breaking have now been observed—microscopic chiral symmetry breaking in freely suspended smectic films and macroscopic chiral symmetry breaking in Langmuir monolayers. Thus, to understand the textures observed in these films, one must consider order on a wide range of length scales.

We thank R. F. Bruinsma, C. M. Knobler, J. M. Schnur, Z.-G. Wang, and J. D. Weeks for many helpful discussions. This research was supported in part by the National Science Foundation through Grant No. DMR-91-03031, and by the Air Force through Grant No. AFOSR-91-0297.

[1] D. K. Schwartz, Nature (London) **352**, 593 (1993).
[2] C. J. Eckhardt *et al.*, Nature (London) **362**, 614 (1993).
[3] R. Viswanathan *et al.*, Nature (London) **368**, 440 (1994).
[4] J. Maclennan and M. Seul, Phys. Rev. Lett. **69**, 2082 (1994); J. E. Maclennan *et al.*, Phys. Rev. E **49**, 3207 (1994).
[5] K. Pang and N. A. Clark, Phys. Rev. Lett. **73**, 2332 (1994).
[6] X. Qiu *et al.*, Phys. Rev. Lett. **67**, 703 (1991).
[7] J. Ruiz-Garcia *et al.*, J. Phys. Chem. **97**, 6955 (1993).
[8] D. K. Schwartz *et al.*, Physica A **204**, 606 (1994).
[9] J. V. Selinger *et al.*, Phys. Rev. Lett. **70**, 1139 (1993).
[10] V. M. Kaganer and E. B. Loginov (unpublished).
[11] R. B. Meyer and P. S. Pershan, Solid State Commun. **13**, 989 (1973).
[12] S. A. Safran *et al.*, Phys. Rev. A **33**, 2186 (1986).
[13] G. A. Hinshaw *et al.*, Phys. Rev. Lett. **60**, 1864 (1988); G. A. Hinshaw and R. G. Petschek, Phys. Rev. A **39**, 5914 (1989).
[14] A. E. Jacobs *et al.*, Phys. Rev. A **45**, 5783 (1992).
[15] S. B. Dierker *et al.*, Phys. Rev. Lett. **56**, 1819 (1986).
[16] O. D. Lavrentovich and V. M. Pergamenshchik, Mol. Cryst. Liq. Cryst. **179**, 125 (1990); Phys. Rev. Lett. **73**, 979 (1994); V. M. Pergamenshchik, Phys. Rev. E **47**, 1881 (1993).

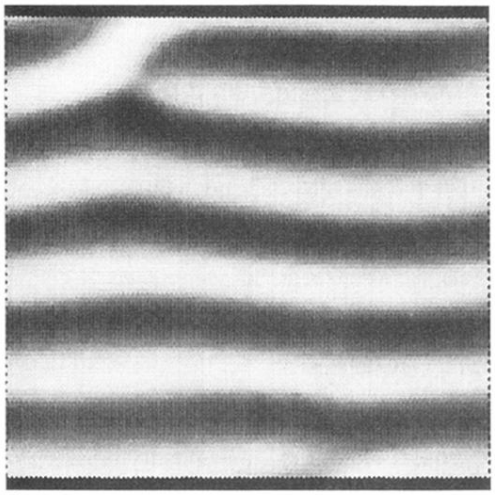

(a)

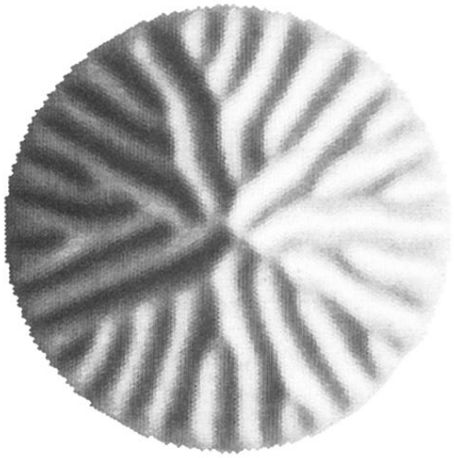

(b)

(c)

FIG. 2. Monte Carlo simulations of (a) the striped phase, (b) a vortex defect with a dense branching morphology, and (c) a spiral defect. The gray scale shows the y component of $\mathbf{c}$. Simulation (a) was done on a hexagonal lattice of 100×110 sites with periodic boundary conditions; (b) and (c) were done on a hexagonal lattice with a circular geometry with a radius of 85 sites.